Earthquakes and Structures, *Vol. 11, No. 2 (2016) 297-313*
DOI: http://dx.doi.org/10.12989/eas.2016.11.2.297

A virtual parameter to improve stability properties for an integration method

Shuenn-Yih Chang*

Department of Civil Engineering National Taipei University of Technology NTUT Box 2653, Taipei 106, Taiwan, Republic of China

(Received September 26, 2014, Revised July 27, 2016, Accepted July 29, 2016)

Abstract. A virtual parameter is introduced into the formulation of the previously published integration method to improve its stability properties. It seems that the numerical properties of this integration method are almost unaffected by this parameter except for the stability property. As a result, it can have second order accuracy, explicit formulation and controllable numerical dissipation in addition to the enhanced stability property. In fact, it can have unconditional stability for the system with the instantaneous degree of nonlinearity less than or equal to the specified value of the virtual parameter for the modes of interest for each time step.

Keywords: unconditional stability; conditional stability; nonlinear dynamic analysis; virtual parameter; structure-dependent integration method

1. Introduction

Recently, a family of structure-dependent integration methods has been successfully developed for structural dynamics (Chang 2014), where a single free parameter p is employed to control its numerical properties. It was analytically shown that it can have the unconditional stability, second order accuracy and controllable numerical dissipation for a linear elastic system. In addition, it was also shown that it has high-frequency numerical damping to suppress or even eliminate the spurious oscillations of high frequency responses while the low frequency responses can be very accurately integrated. Furthermore, it was numerically illustrated that it is very computationally efficient in the step-by-step solution of an inertial problem when compared to the currently available dissipative, implicit integration methods, such as the Wilson θ method (Bathe and Wilson 1973), HHT -α method (Hilber *et al*. 1977), WBZ -α method (Wood *et al*. 1981), generalized -α method (Chung and Hulbert 1993), Bathe implicit method (Bathe and Noh 2012) and the methods developed by Zhou and Tamma (2006). Consequently, it seems that this family method is very competitive with the currently available integration methods. However, numerical experiments reveal that instability may occur in the step-by-step solution of a nonlinear system although it has been verified that it can have unconditional stability for a linear elastic system.

*Corresponding author, Professor, E-mail: changsy@ntut.edu.tw

http://www.techno-press.com/journals/eas&subpage=7 ISSN: 2092-7614 (Print), 2092-7622 (Online)

Hence, the stability analysis of this family method for a nonlinear system must be further conducted.

In general, the basic analysis of an integration method for a linear elastic system is performed for a complete a step-by-step integration procedure (Belytschko and Hughes 1983). However, this basic analysis technique for a linear elastic system cannot be applicable to a nonlinear system since the structural properties might vary per time step for a nonlinear system. In order to overcome this difficulty, the technique for the basic analysis of a nonlinear system has been proposed by Chang (2007, 2010), where a novel parameter, which is referred as the instantaneous degree of nonlinearity for a specific time step, is introduced to monitor the stiffness change at the end of the time step. Besides, the basic analysis for a nonlinear system is no longer conducted for a whole integration procedure but for a single time step. This is because that a whole integration procedure consists of each time step. This implies that the numerical properties of an integration method for a single time step can still provide the very useful information for a complete integration procedure. As a result, this technique is adopted in this study.

After the basic analysis of the previously published integration method for a nonlinear system, the cause of the instability will be revealed. Apparently, the application of this integration method to perform a nonlinear dynamic analysis will be inconvenient or even be limited due to instability. Hence, to overcome this difficulty, a virtual parameter is introduced into the general formulation of the integration method. It will be shown that an appropriate choice of this parameter can effectively avoid the stability problem. In addition, the numerical properties of this integration method can be preserved. All the details will be present in this work.

2. Previously published method

A family of dissipative, explicit, structure-dependent integration method has been developed for time integration and it can be expressed as

$$\begin{aligned} & ma_{i+1} + c_0 v_{i+1} + \frac{2p}{p+1} k_{i+1} d_{i+1} - \frac{p-1}{p+1} k_i d_i = \frac{2p}{p+1} f_{i+1} - \frac{p-1}{p+1} f_i \\ & d_{i+1} = \beta_0 d_{i-1} + \beta_1 d_i + \beta_2 (\Delta t) v_i + \beta_3 (\Delta t)^2 a_i \\ & v_{i+1} = v_i + \frac{3p-1}{2(p+1)} (\Delta t) a_i - \frac{p-3}{2(p+1)} (\Delta t) a_{i+1} \end{aligned} \tag{1}$$

where m and c_0 are the mass and viscous damping coefficient, respectively; k_i is the stiffness at the end of the *i-th* time step. In addition, d_i, v_i, a_i and f_i are the nodal displacement, velocity, acceleration and external force at the end of the *i-th* time step, respectively. The coefficients β_0 to β_3 are found to be

$$\begin{aligned} \beta_0 &= -\frac{1}{D}\left[\frac{p-1}{8}\left(\frac{2}{p+1}\right)^3 \Omega_0^2\right] & \beta_1 &= 1 + \frac{1}{D}\left[\frac{p-1}{8}\left(\frac{2}{p+1}\right)^3 \Omega_0^2\right] \\ \beta_2 &= \frac{1}{D}\left(1 - \frac{p-3}{p+1}\xi\Omega_0\right) & \beta_3 &= \frac{1}{D}\left\{\tfrac{1}{2} - \tfrac{1}{2}\left[\left(\frac{2}{p+1}\right)^2 + \frac{p-3}{p+1}\right]\xi\Omega_0\right\} \end{aligned} \tag{2}$$

where ξ is a viscous damping ratio; $\Omega_0=\omega_0(\Delta t)$ and $\omega_0=\sqrt{k_0/m}$ is the natural frequency of the system determined from the initial stiffness k_0. In addition, p is the parameter to govern the numerical properties and D is found to be

$$D=1-\frac{p-3}{p+1}\xi\Omega_0+\frac{p}{4}\left(\frac{2}{p+1}\right)^3\Omega_0^2 \tag{3}$$

For brevity, the family of the previously published integration methods will be referred as PM since this method is controlled by the "p" parameter.

3. Basic analysis for nonlinear system

In order to conduct the basic analysis of PM for a nonlinear system, a parameter is introduced to monitor the stiffness change and is called the instantaneous degree of nonlinearity (Chang 2007). It is defined as the ratio of the stiffness at the end of the *i-th* time step over the initial stiffness and is

$$\delta_i=\frac{k_i}{k_0} \tag{4}$$

It is clear that δ_i=1 implies the instantaneous stiffness at the end of the *i-th* time step equal to the initial stiffness. Whereas, the case of δ_i>1 implies that the instantaneous stiffness is larger than the initial stiffness at the end of the *i-th* time step; and the case of 0<δ_i<1 implies that the instantaneous stiffness is less than the initial stiffness.

After introducing δ_i to monitor the stiffness change, the use of PM to calculate the free vibration response of a single degree of freedom system can be expressed as

$$\mathbf{X}_{i+1}=\mathbf{A}_{i+1}\mathbf{X}_i \tag{5}$$

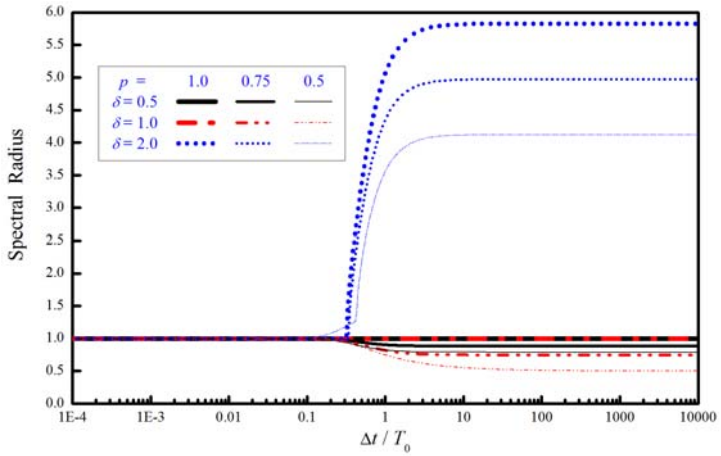

Fig. 1 Variation of spectral radius with $\Delta t/T_0$

where $\mathbf{X}_i=[d_i, (\Delta t)v_i, (\Delta t)^2 a_i]^{\mathrm{T}}$ is defined; and $\mathbf{A}_{i+1}$ is the amplification matrix of PM at the end of the $(i+1)$-*th* time step. Notice that $\mathbf{A}_{i+1}$ might vary for each time step for a nonlinear system. As a result, the explicit expression of $\mathbf{A}_{i+1}$ is found to be

$$\mathbf{A}_{i+1}=\begin{bmatrix} A_{11} & A_{12} & A_{13} \\ A_{21} & A_{22} & A_{23} \\ A_{31} & A_{32} & A_{33} \end{bmatrix} \tag{6}$$

where

$$\begin{aligned}
&A_{11}=\beta_1+\frac{2p}{p-1}\beta_0 \quad , \quad A_{12}=\beta_2+\frac{p+1}{p-1}\frac{2\beta_0\xi\Omega_0}{\Omega_i^2} \quad , \quad A_{13}=\beta_3+\frac{p+1}{p-1}\frac{\beta_0}{\Omega_i^2} \\
&A_{21}=\frac{\Omega_{i+1}^2}{B}\frac{3-p}{2(p+1)}\left(\frac{p-1}{p+1}-\frac{2p}{p+1}\beta_1-\frac{4p^2}{p+1}\frac{1}{p-1}\beta_0\right) \\
&A_{22}=\frac{1}{B}\left(1-\frac{p}{p+1}\frac{3-p}{p+1}\beta_2\Omega_{i+1}^2-\frac{p}{p-1}\frac{3-p}{p+1}\frac{2\beta_0\xi\Omega_0\Omega_{i+1}^2}{\Omega_i^2}\right) \\
&A_{23}=\frac{1}{B}\left(\frac{3p-1}{2(p+1)}-\frac{p}{p+1}\frac{3-p}{p+1}\beta_3\Omega_{i+1}^2-\frac{p}{p-1}\frac{3-p}{p+1}\frac{\beta_0\Omega_{i+1}^2}{\Omega_i^2}\right) \\
&A_{31}=\frac{\Omega_{i+1}^2}{B}\left(\frac{p-1}{p+1}-\frac{2p}{p+1}\beta_1-\frac{2p}{p-1}\frac{2p}{p+1}\beta_0\right) \\
&A_{32}=-\frac{1}{B}\left(2\xi\Omega_0+\frac{2p}{p+1}\beta_2\Omega_{i+1}^2+\frac{2p}{p-1}\frac{2\beta_0\xi\Omega_0\Omega_{i+1}^2}{\Omega_i^2}\right) \\
&A_{33}=-\frac{1}{B}\left(\frac{3p-1}{p+1}\xi\Omega_0+\frac{2p}{p+1}\beta_3\Omega_{i+1}^2+\frac{2p}{p-1}\frac{\beta_0\Omega_{i+1}^2}{\Omega_i^2}\right)
\end{aligned} \tag{7}$$

where $B=1-(p-3)/(p+1)\xi\Omega_0$.

The characteristic equation of the matrix $\mathbf{A}_{i+1}$ can be obtained from $|\mathbf{A}_{i+1}-\lambda\mathbf{I}|=0$. As a result, it is found to be

$$\lambda^3-A_1\lambda^2+A_2\lambda-A_3=0 \tag{8}$$

where λ is an eigenvalue of $\mathbf{A}_{i+1}$. It is very complicated to explicitly derive the coefficients A_1, A_2 and A_3. However, the numerical properties of PM can be numerically obtained from Eq. (8) without using the explicit expressions of the coefficients A_1, A_2 and A_3.

The variations of spectral radii with $\Delta t/T_0$ for different instantaneous degree of nonlinearity δ_i and δ_{i+1} as well as different p values are plotted in Fig. 1. It is apparent that there are many combinations of δ_i and δ_{i+1} for simulating a variety of nonlinear cases. However, for brevity but without losing generality the cases of $\delta_i=\delta_{i+1}=\delta=0.5$, 1.0 and 2.0 are considered since δ_i is, in general, close to δ_i for the consecutive time steps in an integration procedure. In addition, the cases of $p=1$, 0.75 and 0.50 are considered. The spectral radius is always less than or equal to 1 for $\delta=0.5$ and 1.0 and finally approaches a constant smaller than or equal to 1 while it becomes greater than

1 for δ=2.0 and finally tends to a constant greater than 1. It is revealed by further numerical experiments that the spectral radius is always less than or equal to 1 for $\delta \leq 1$ while it becomes greater than 1 for $\delta > 1$. Hence, it can be concluded that PM is unconditionally stable for $\delta \leq 1$ while it is conditionally stable for $\delta > 1$.

4. A virtual parameter

Since PM can only have conditional stability for $\delta > 1.0$, its application to conduct a nonlinear dynamic analysis may be inconvenient or even limited. There is a motive to improve the stability properties of PM by virtually introducing a parameter σ into the coefficients of β_0 to β_3. The motivation of this technique and implementation details will be presented in this section.

It was shown in the previous section that PM is unconditionally stable in the range of $\delta \leq 1$ while it becomes conditionally stable in the range of $\delta > 1$. On the other hand, in the formulation of PM, only the coefficients β_0 to β_3 are functions of the initial stiffness k_0. Both combines to imply that PM can have unconditionally stable only if the instantaneous stiffness k is equal to or less than the initial stiffness k_0, i.e., $\delta \leq 1$. Hence, based on this characteristic, the unconditional stability range of PM can be enlarged if the initial stiffness is visually modified from k_0 to σk_0 by the virtual parameter σ. As a result, the unconditional stability range alters from $k \leq k_0$ to $k \leq \sigma k_0$ since PM is unconditionally stable only if $\delta \leq 1$ is satisfied. Hence, it is implied that an unconditional stability range can be enlarged if σ is chosen to be greater than 1. Whereas, it will be shrunk if $0 < \sigma < 1$ is adopted.

To apply the virtual parameter σ to PM, its formulation can also be expressed as shown in Eq. (1). However, the coefficients β_0 to β_3 must be modified and become

$$\begin{aligned} \beta_0 &= -\frac{1}{D}\left[\frac{p-1}{8}\left(\frac{2}{p+1}\right)^3 \sigma\Omega_0^2\right] & \beta_1 &= 1+\frac{1}{D}\left[\frac{p-1}{8}\left(\frac{2}{p+1}\right)^3 \sigma\Omega_0^2\right] \\ \beta_2 &= \frac{1}{D}\left(1-\frac{p-3}{p+1}\xi\Omega_0\right) & \beta_3 &= \frac{1}{D}\left\{\tfrac{1}{2}-\tfrac{1}{2}\left[\left(\frac{2}{p+1}\right)^2+\frac{p-3}{p+1}\right]\xi\Omega_0\right\} \end{aligned} \tag{9}$$

where D becomes

$$D = 1-\frac{p-3}{p+1}\xi\Omega_0+\frac{p}{4}\left(\frac{2}{p+1}\right)^3 \sigma\Omega_0^2 \tag{10}$$

Notice that although the numerators of β_2 and β_3 remain unchanged as shown in Eq. (9), their denominator D varies.

In order to gain an insight into the stability conditions of PM with the inclusion of the virtual parameter σ, the variation of upper stability limit with the instantaneous degree of nonlinearity is plotted in Figs. 2 and 3 for p=0.1 and 0.5, respectively. It is manifested from Fig. 2 that the unconditional stability range is found to be $\delta \leq 1$, $\delta \leq 2$ and $\delta \leq 3$ corresponding to the value of σ=1, 2 and 3 for the different viscous damping ratios of ξ=0, 0.1 and 0.2. This implies that the

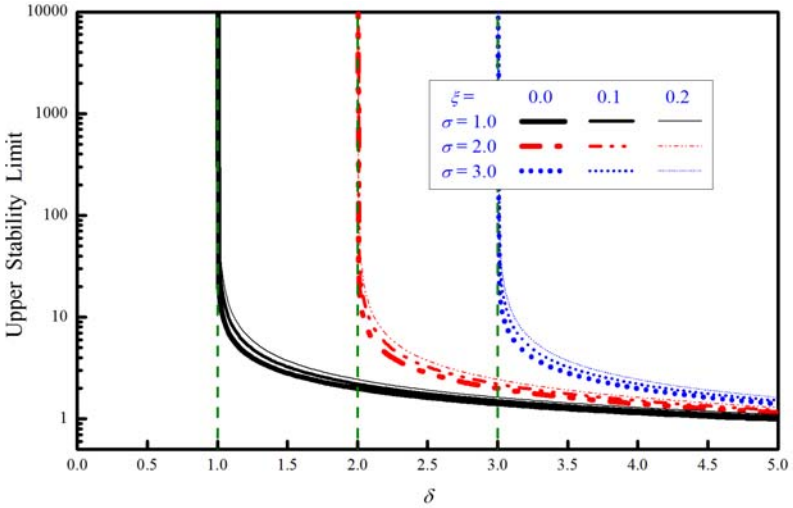

Fig. 2 Variation of upper stability limit with δ for PM with p=1.0

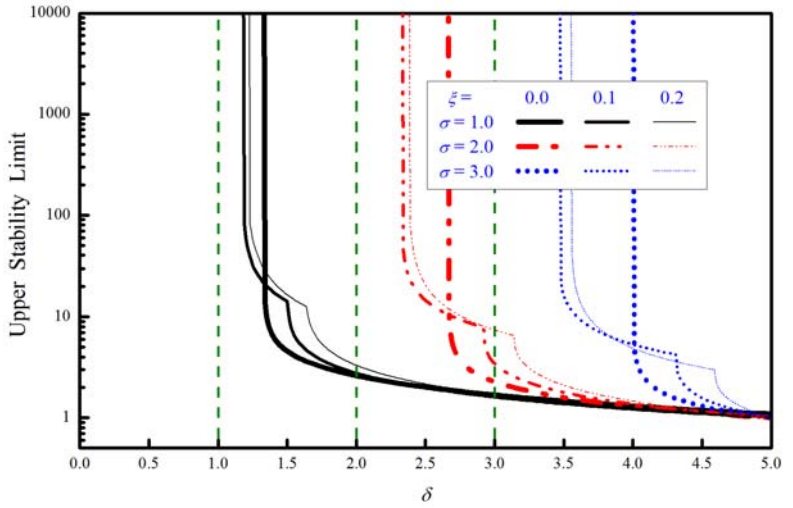

Fig. 3 Variation of upper stability limit with δ for PM with p=0.5

introduction of σ into PM can extend its unconditional stability range from $\delta \le 1$ to $\delta \le \sigma$ and it becomes conditionally stable in the range of $\delta > \sigma$. The case of σ=1 implies that there is no inclusion of the virtual parameter σ for PM. Very similar phenomena are also found in Fig. 3 for the case of p=0.5. However, it is seen in this figure that the virtual parameter σ seems to extend the unconditional stability range to be larger than that of $\delta_{i+1} \le \sigma$. In fact, it is to extend from $\delta \le 1$ to $\delta \le \bar{\sigma}$, where $\bar{\sigma} \ge \sigma$. Notice that there is a bifurcation point in the curves for ξ=0.1 and 0.2 in Fig. 3, where the real, distinct principal eigenvalues bifurcate into complex conjugate eigenvalues. Both Figs. 2 and 3 confirm that the virtual parameter σ can alter the unconditional stability range from $\delta \le 1$ to $\delta \le \sigma$. This implies that a large value of σ leads to a large unconditional stability range. Since it is seldom experienced that the instantaneous stiffness of a real structure is larger than twice of

the initial stiffness, i.e., δ>2. Thus, the case of $\delta \leq 2$ is considered in this study since this range may be large enough for practical applications.

5. Numerical properties of PM with virtual parameter

The coefficients of β_0 to β_3 for PM are modified after introducing the virtual parameter σ. Although this parameter can enhance the stability properties of PM, the other numerical properties of PM might also be affected by this parameter. Hence, the numerical properties of PM with the inclusion of σ must be further evaluated.

5.1 Spectral radius

The variations of spectral radii with $\Delta t/T_0$ for PM with σ=2 are shown in Fig. 4. The spectral radius is always less than or equal to 1 for each curve of this figure. This is consistent with the analytical prediction that the application of the virtual parameter σ to PM can extend the unconditional stability range from $\delta \leq 1$ to $\delta \leq \sigma$. In general, each curve has a unit spectral radius for small $\Delta t/T_0$ while it decreases gradually and finally tends to a certain constant less than 1. It is also found that the constant value decreases with the decrease of p for given δ and $\Delta t/T_0$. Whereas, it decreases with the increase of δ for given p and $\Delta t/T_0$ if $p \neq 1.0$.

5.2 Relative period error

Variations of relative period errors with $\Delta t/T_0$ are shown in Fig. 5. In general, the relative period error increases with the increase of $\Delta t/T_0$ as δ and p are given. Period elongation is generally found for PM and its amount increases with the decrease of p for a given δ while it is

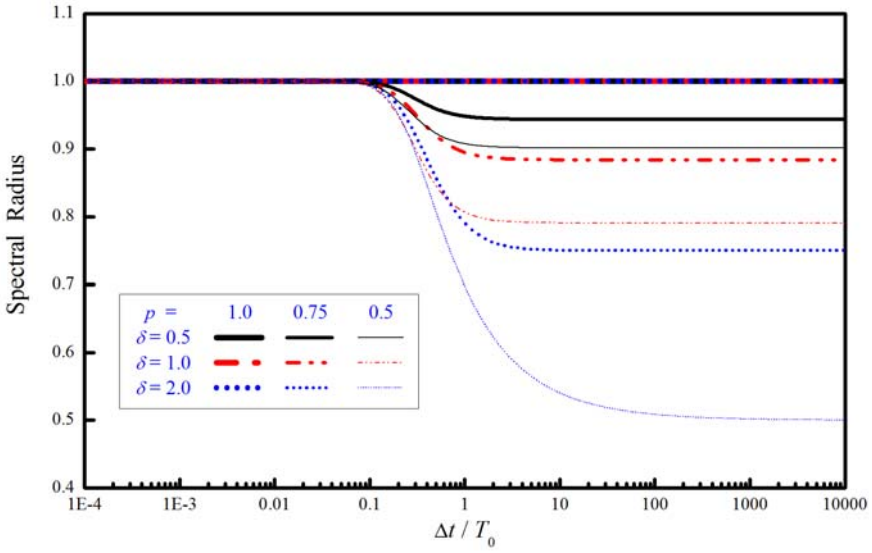

Fig. 4 Variation of spectral radius with $\Delta t/T_0$ for PM with σ=2

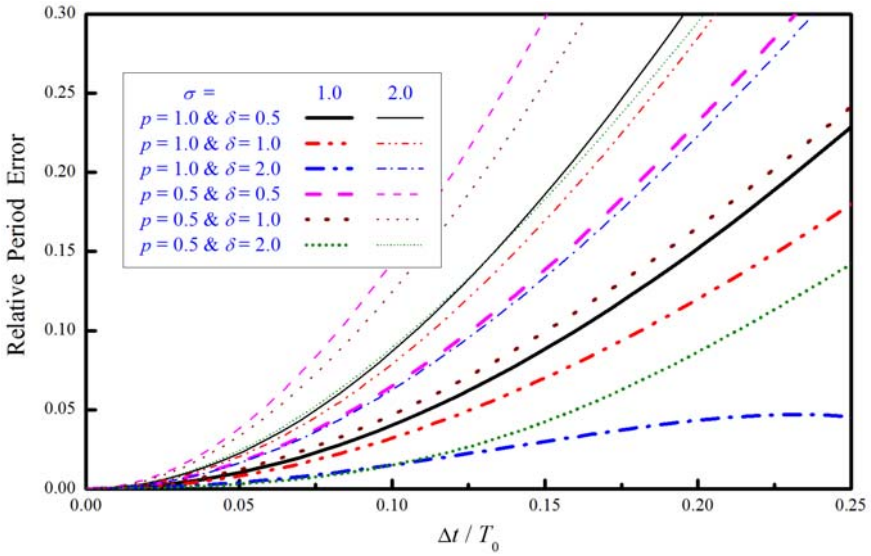

Fig. 5 Variation of relative period error with $\Delta t/T_0$

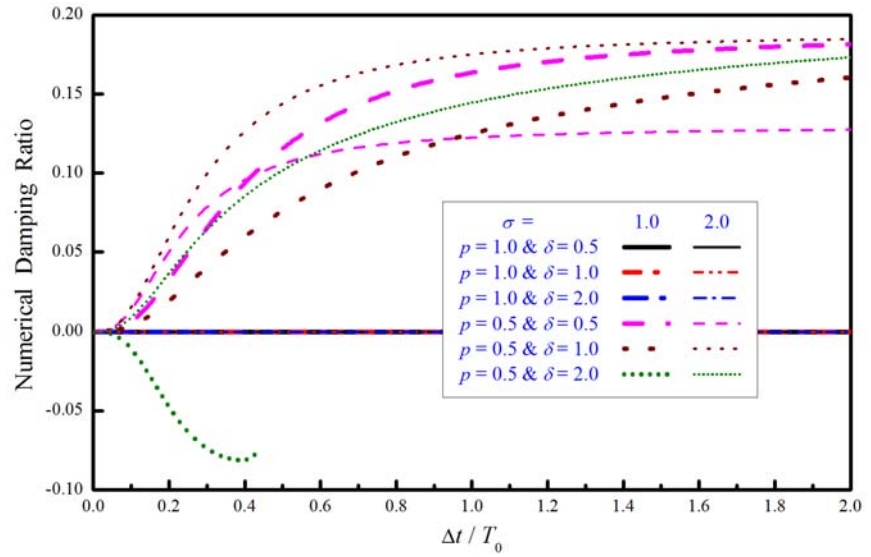

Fig. 6 Variation of numerical damping ratio with $\Delta t/T_0$

decreased with the increase of δ for a given p. It is also found that the relative period error for the case of σ=2 is, in general, larger than that of the case of σ=1 for a small value of $\Delta t/T_0$ for the given p and δ values. Numerical experiments also reveal that the increase of σ results in the increase of period distortion. Thus, although a large σ can extend the unconditional stability range from $\delta \leq 1$ to $\delta \leq \sigma$, it leads to more period distortion. In this figure, the relative period error is small for $\Delta t/T_0 \leq 0.05$ for σ=1 while $\Delta t/T_0 \leq 0.025$ may be needed for σ=2 to have roughly the same period distortion. Consequently, the increase of σ value will increase the unconditional stability range but will sacrifice the numerical accuracy.

5.3 Numerical damping

Fig. 6 shows the variations of numerical damping ratios with $\Delta t/T_0$ for PM. It is clear that there is no numerical dissipation for the case of p=0.1 for both σ=1 and 2. Whereas, the case of p=0.5 generally leads to favorable numerical dissipation except for the case of σ=1 and δ=2. In general, the numerical damping ratio increases with $\Delta t/T_0$ and finally approached a constant value for PM with p=0.5 as $\delta \leq 1$ while a negative damping ratio is found for the case of σ=1 and δ=2. This is because that instability occurs for σ=1 and δ=2. As a summary, a favorable numerical dissipation property can be obtained from PM with an appropriate value of $\sigma \geq 1$ and the choice of $1/2 \leq p < 1.0$ if $\delta \leq \sigma$ is satisfied during the integration procedure.

5.4 Overshooting

Overshooting is adverse to an integration method (Goudreau and Taylor 1972, Hilber and Hughes 1978). The behavior as $\Omega_i \to \infty$ gives an indication of the behavior of the high frequency mode for a system where the values of $\Delta t/T_i$ are large for the high-frequency modes. Employing Eq. (5) with the matrix $\mathbf{A}_{i+1}$, one can have the following equations for the limiting condition of $\Omega_i \to \infty$

$$\begin{aligned} d_{i+1} &\approx \left[1 - \frac{(p+1)^3 \delta_i}{4p}\right] d_i \\ v_{i+1} &\approx -\left[\frac{(p+1)(p-3)\delta_i \delta_{i+1}}{4} + 1 + \frac{p-3}{2(p+1)}(\delta_i - \delta_{i+1})\right] \Omega_0 \omega_0 d_i + \left[1 + \frac{(p+1)(p-3)\delta_{i+1}}{2}\right] v_i \end{aligned} \tag{11}$$

Notice that both d_{i+1} and v_{i+1} are independent of σ in this equation. Thus, it is implied that the overshooting behaviors of PM are not affected by the virtual parameter σ. The first line of this equation reveals that there is s no overshoot in displacement for any member of PM while it generally has a tendency to overshoot linearly in Ω_0 in the velocity equation due to the initial displacement term.

In order to examine the overshoot behavior of PM affected by σ, the discrete displacement and velocity responses are obtained from PM with p=1 and 0.5 for σ=2. The free vibration response to the initial conditions d_0=1 and v_0=0 is calculated with the time step of $\Delta t/10T_0$. To simulate the system with different stiffness characteristic, the stiffness is assumed to be in the form of $k=k_0(1+\theta u^2)$. Hence, the cases of θ=0, -0.1 and 1 will lead to δ=1, δ<1 and δ>1 for each time step correspondingly. Numerical results are shown in Fig. 7. For comparison, the results obtained from the constant average acceleration method (AAM) (Newmark 1959) are also plotted in this figure. The velocity term is normalized by the initial natural frequency of the system in order to have the same unit as displacement. It is seen in Figs. 7(a), 7(c) and 7(e) that PM with p=1 or 0.5 for σ=2 shows no overshoot in displacement for δ=1, δ<1 and δ>1. However, a significant overshoot in velocity is found in Figs. 7(b), 7(d) and 7(f). As a summary, the phenomena of overshoot both in displacement and velocity for PM with p=1 or 0.5 for σ=2 are consistent with the analytical results shown in Eq. (11).

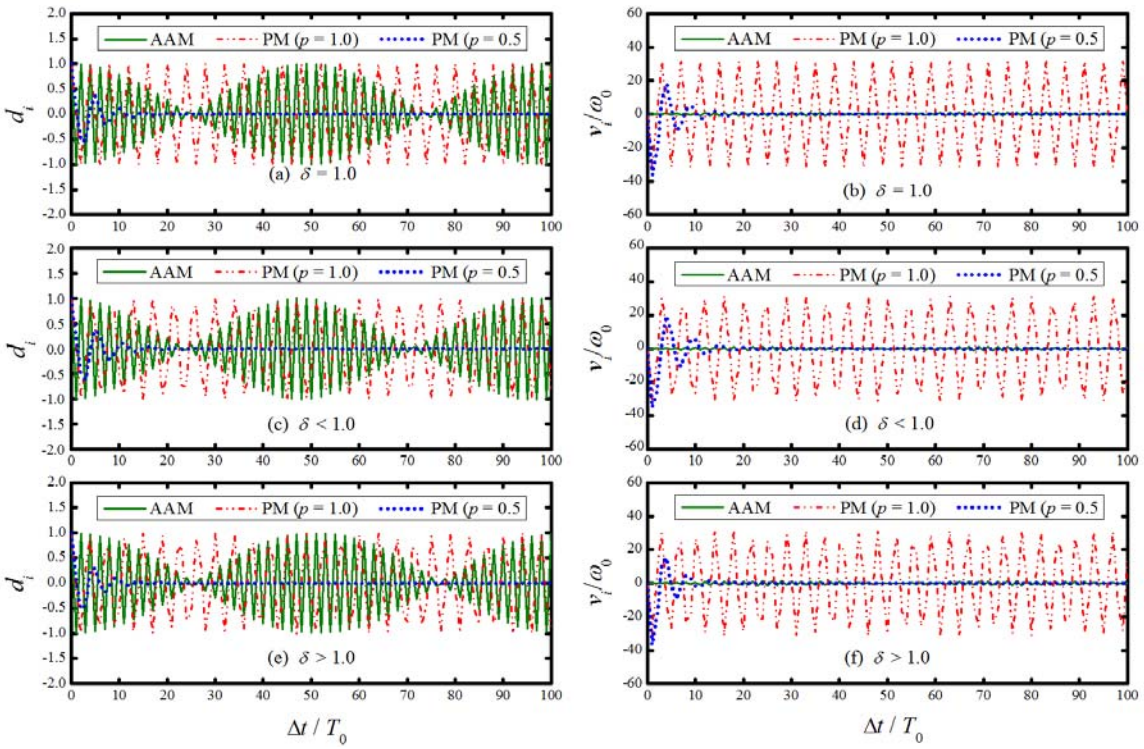

Fig. 7 Comparisons of overshoot responses for PM

6. Numerical illustrations

Notice that the implementation details of PM is almost unaffected by the application of the virtual parameter σ into its formulation. An example is used to examine the numerical properties of PM. In fact, the numerical properties of unconditional stability, accuracy and numerical damping are addressed. For brevity, the specified values of p and σ corresponding to PM1 to PM4 are listed in Table 1. In addition, their unconditional stability range and numerical damping property are also shown in this table. In the following numerical illustration, a two-story shear-beam building is considered and is shown in Fig. 8. The bending stiffness of each story is

$$k = k_0\left[1 + h\left(\Delta u\right)^2\right] \tag{12}$$

where k_0 is the initial stiffness and Δu is a story drift. The nonlinear stiffness term will appear for $h \neq 0$. Based on the initial stiffness matrix, the natural frequencies of the system are found to be $\omega_0^{(1)} = 3.16$ and $\omega_0^{(2)} = 1000.00$ *rad/sec*; and their corresponding modal shapes are

$$\phi_1 = \begin{Bmatrix} 1 \\ 10^4 \end{Bmatrix} \qquad \phi_2 = \begin{Bmatrix} 1 \\ -10^{-4} \end{Bmatrix} \tag{13}$$

It is clear that the two modes are widely separated from each other. Meanwhile, in order to simulate the system with δ=1, δ<1 and δ>1, three sets with different values of h_1 and h_2 are

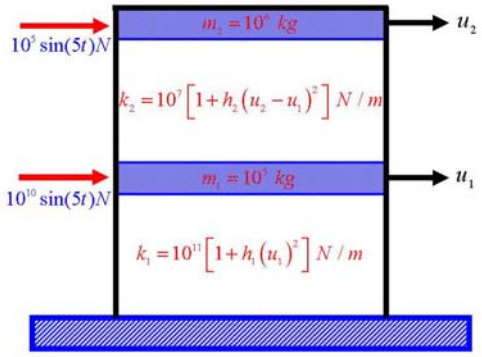

Fig. 8 A 2-story shear-beam type building

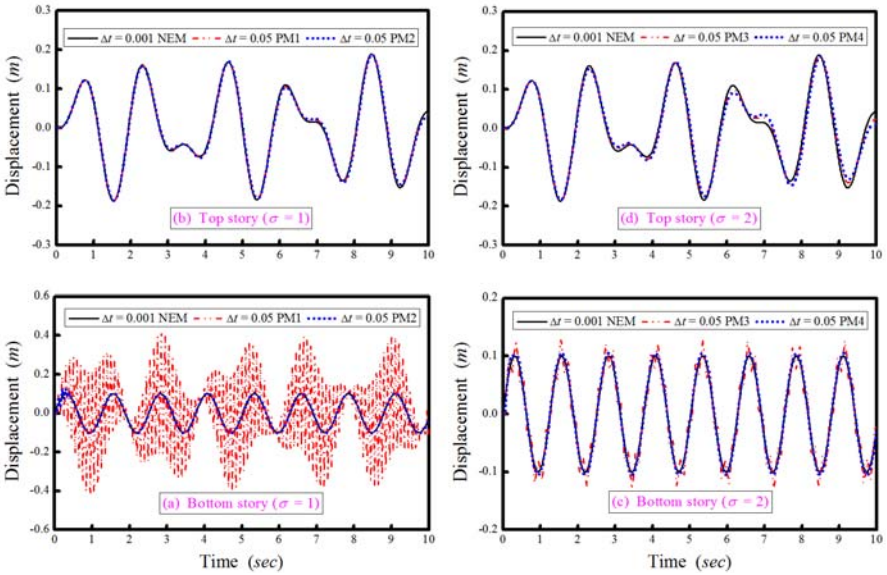

Fig. 9 Displacement responses of System-A

Table 1 Four specific members of PM

Member	p	σ	Unconditional Stability Range	Numerical Damping
PM1	1.0	1	$\delta \le 1$	No
PM2	0.5	1	$\delta \le 1$	Yes
PM3	1.0	2	$\delta \le 2$	No
PM4	0.5	2	$\delta \le 2$	Yes

specified and they are

System-A $h_1 = h_2 = 0$ $\delta = 1$ for each mode and time step

System-B $h_1 = h_2 = -0.5$ $\delta < 1$ for each mode and time step

System-C $h_1 = h_2 = 1$ $\delta > 1$ for each mode and time step

These three systems are subjected to the same applied loads as shown in Fig. 8. For comparison, the displacement response obtained from NEM with Δt=0.001 *sec* is considered as a reference solution for comparison. Meanwhile, numerical results are also obtained from PM1 to PM4 with Δt=0.05 *sec* for all the three systems. Figs. 9 to 11 show the numerical results for System-A, System-B and System-C, respectively.

6.1 Responses to System-A

Since h_1=h_2=0 is taken for System-A, thus this system is a linear elastic system. In Fig. 9, it seems that PM1 to PM4 can generally provide reliable solutions for the top story. Whereas, for the bottom story, only PM2 and PM4 can give acceptable results while those obtained from PM1 and PM3 are unacceptable. It is indicated that PM1 to PM4 can have unconditional stability for δ=1 since they all lead to stable solutions and the value of $\omega_0^{(2)}(\Delta t)$ is as large as 50. Notice that the second mode is a very high frequency mode; and it contributes significantly to the bottom story while its contribution to the top story is negligible, which can be manifested from ϕ_2 as shown in Eq. (13). In addition, the time step of Δt=0.05 *sec* is able to accurately integrate the first mode while it will lead to a very significant period distortion for the second mode. Since there is no contribution from the second mode to the top story, thus PM1 to PM4 can give accurate results for the top story. It is apparent that the results obtained from PM1 and PM3 for the bottom story are contaminated by the second mode. Since the numerical damping of PM2 and PM4 can be used to filter out the spurious oscillations of the second mode very early, the results obtained from PM2 and PM4 for the bottom story are reliable.

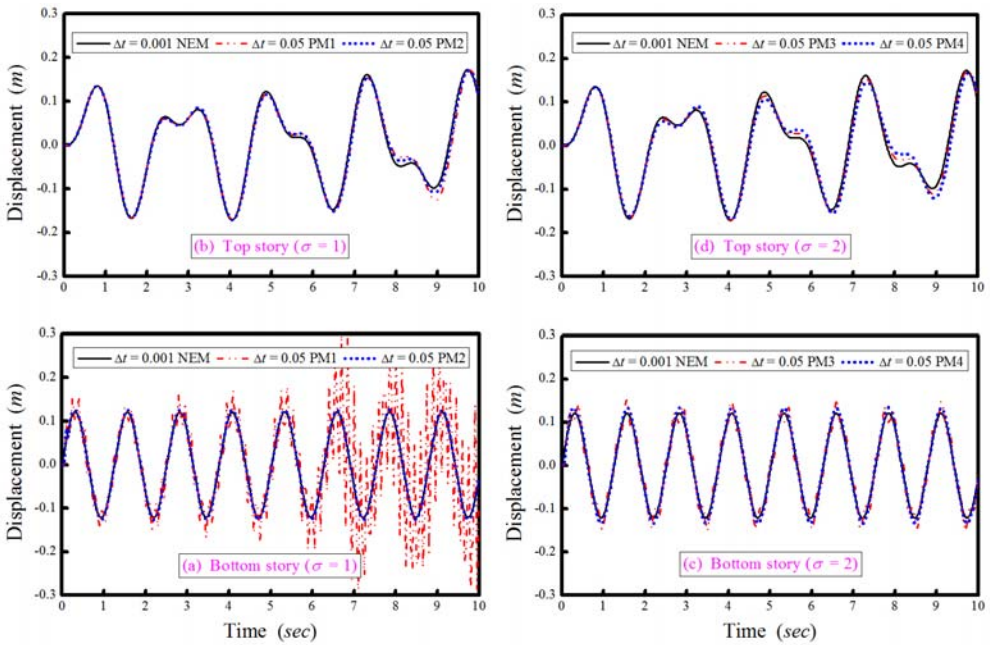

Fig. 10 Displacement responses of System-B

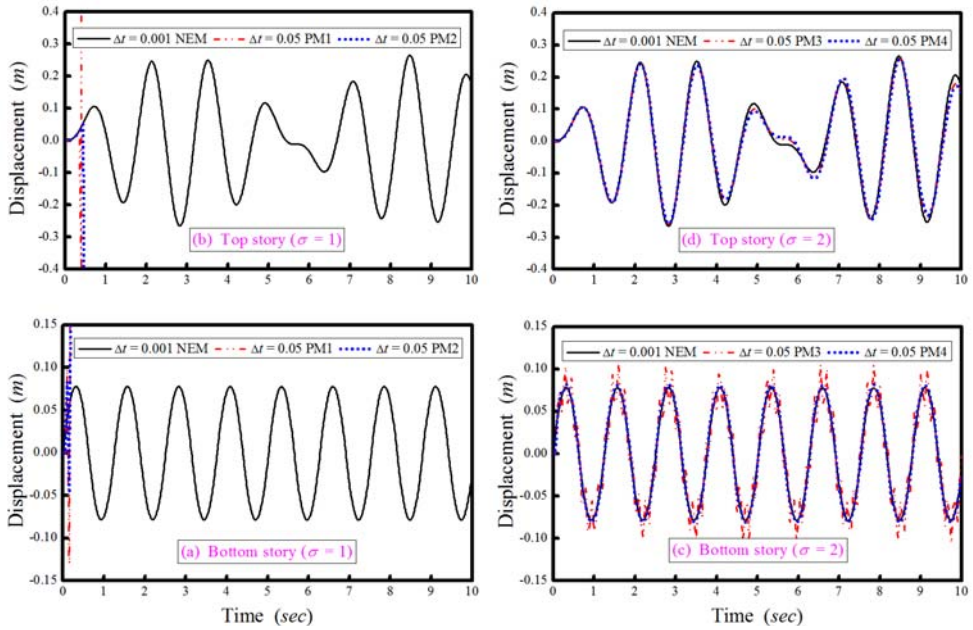

Fig. 11 Displacement responses of System-C

6.2 Responses to System-B

In order to show that System-B always leads to $\delta<1$ and System-C always leads to $\delta>1$ for each mode and each time step, the technique to evaluate the instantaneous degree of nonlinearity for each mode is described next. It is recognized that a nonlinear multiple degree of freedom system cannot reduce to uncoupled single degree of freedom systems for a complete integration procedure. However, it can be done for each time step and thus the numerical properties for the solution of a nonlinear single degree of freedom system can be used to these uncoupled single degree of freedom systems. This relies upon the natural frequencies of the modes of interest in each time step since the instantaneous degrees of nonlinearity for these modes can be determined from these frequencies. In fact, the instantaneous degree of nonlinearity at the *i-th* time step for the *j-th* mode can be calculated by the following equation after finding the natural frequency of the *j-th* mode at the *i-th* time step

$$\delta_i^{(j)} = \left[\frac{\omega_i^{(j)}}{\omega_0^{(j)}} \right]^2 \tag{14}$$

where $\omega_0^{(j)}$ and $\omega_i^{(j)}$ are the natural frequencies of the *j-th* mode based on the initial stiffness and the stiffness at the end of the *i-th* time step. Based on Eq. (14), the time histories of the instantaneous degree of nonlinearity for the two modes of System-B and System-C are plotted in Figs. 12 and 13, respectively.

Fig. 12 reveals that $\delta_i^{(1)}$ varies between 0.7 and 1.0 and $\delta_i^{(2)}$ varies between 0.6 and 1.0. Hence, it is confirmed that $\delta<1$ for each mode and each time step for System-B. Consequently, the unconditional stability of PM1 to PM4 for $\delta<1$ is indicated since they lead to stable results

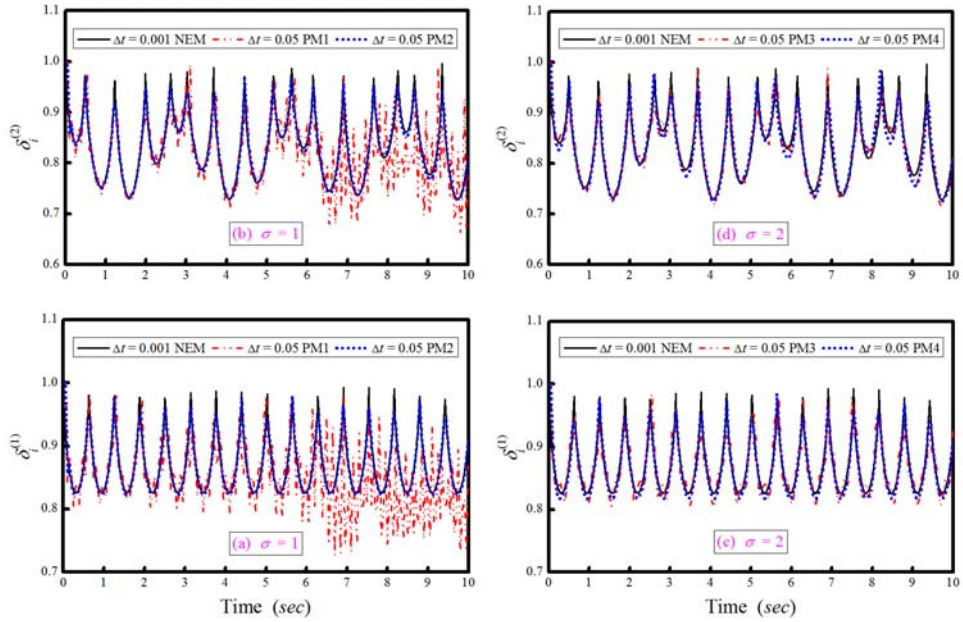

Fig. 12 Time history of instantaneous degree of nonlinearity for System-B

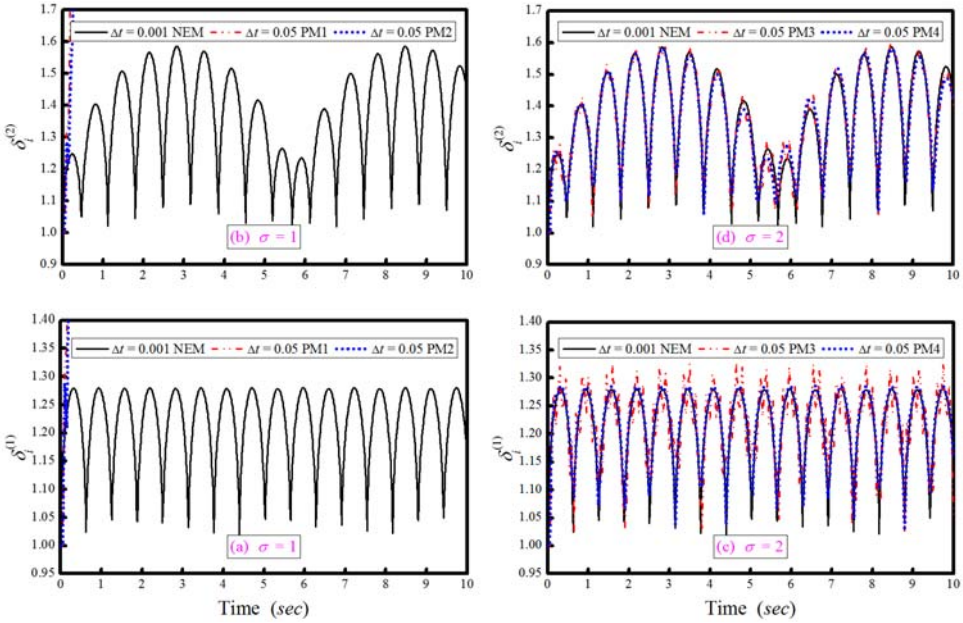

Fig. 13 Time history of instantaneous degree of nonlinearity for System-C

although the results obtained from PM1 and PM3 significantly deviate from the reference solutions. Since the phenomena and the causes of these phenomena for the numerical results obtained from PM1 to PM4 are very similar to those found in Fig. 9, thus they will not elaborated

here again.

6.3 Responses to System-C

It is seen in Fig. 13 that $\delta_i^{(1)}$ varies between 1.0 and 1.35 and $\delta_i^{(2)}$ varies between 1.0 and 1.6. Hence, it is confirmed that $\delta>1$ for each mode and each time step for System-C. Figs. 11(a) and 11(b) reveal that the results obtained from PM1 and PM2 blow up very early. This is consistent with the analytical results, which reveal that PM1 and PM2 can only have unconditional stability for $\delta\leq1$ while they become conditionally stable for $\delta>1$. Thus, the violation of the upper stability limit is responsible for the numerical instability for PM1 and PM2. On the other hand, in Figs. 11(c) and 11(d), it is seen that PM3 and PM4 result in stable solutions. This attests to that the application of $\sigma=2$ to PM can enlarge the unconditional stability range from $\delta\leq1$ to $\delta\leq2$. In addition, PM4 gives reliable solutions for both top and bottoms stories; while PM3 only provides reliable solution for the top story while the result for the bottom story deviates from the reference solution. This can be explained by next. Since PM3 has no numerical damping to suppress the second mode response, thus the bottom story response is contaminated by this response. On the other hand, the numerical damping of PM4 is able to effectively filter out the second mode response and thus PM4 leads to a reliable solution.

7. Summarized numerical properties

After introducing the virtual parameter $\sigma=2$ into PM, it can have unconditional stability in the range of $\delta\leq2$, which is large enough for practical applications. Thus, the stability problem no longer limit the application of this integration method or cause any inconvenience. Notice that all the other numerical properties of PM are unaffected by this modification. Hence, the modified PM can integrate unconditional stability, explicit formulation, second-order accuracy and controllable numerical damping together. As a result, it is very competitive to the traditional implicit integration methods, such as the Newmark method, HHT-α method, WBZ-α method and generalized-α method. When compared to these implicit integration method, the most important improvement of this integration method is the simultaneous integration of explicit formulation and unconditional stability. In general, it will involve no nonlinear iterations due to the explicit formulation of each time step while there is no limitation on step size due to unconditional stability. Thus, a relatively large time step might be adopted to carry out the time integration without involving an iteration procedure. On the other hand, an iteration procedure is often involved for each time step for the implicit integration methods although they can also have unconditional stability. Notice that it is very time consuming for involving the nonlinear iterations of each time step. Consequently, PM is much more computationally efficient when compared to these implicit integration methods. It has been shown in the reference (Chang 2014) that the CPU time consumed by PM may be as small as 1% of that consumed by the constant average acceleration method for a 1000-degree-of-freedom system. Since this improved integration method can have desired numerical dissipation, such as that possessed by the HHT-α method, WBZ-α method and generalized-α method, thus it is very promising for solving inertial problems, where the total response is dominated by low frequency modes while high frequency responses are of no interest.

8. Conclusions

It is numerically illustrated and analytically verified that the previously published integration method may lead to numerical instability in the solution of a nonlinear system. In fact, it is shown that this integration method can only have unconditional stability for $\delta \leq 1$ and it will become conditionally stable for $\delta > 1$. Consequently, its application may become inconvenient or limited in practical applications. In order to overcome this difficulty, a virtual parameter σ is introduced into the formulation of this integration method to improve its stability properties. As a result, its unconditional stability range is effectively extended from $\delta \leq 1$ to $\delta \leq \sigma$. It seems that the choice of $\sigma = 2$ is good enough for practical applications since it is very rare to encounter that for an actual structure, whose instantaneous stiffness is as large as twice of that of the initial stiffness. This improved stability property is very important for practical applications since it can avoid the need to consider the stability problem. It is worth noting that the other numerical properties of this modified integration method are not altered by this modification. Consequently, it can have unconditional stability, second-order accuracy, explicit formulation and favorable numerical dissipation.

Acknowledgements

The author is grateful to acknowledge that this study is financially supported by the National Science Council, Taiwan, R.O.C., under Grant No. NSC-100-2221-E-027-062.

References

Bathe, K.J. and Wilson, E.L. (1973), "Stability and accuracy analysis of direct integration methods", *Earthq Eng. Struct. Dyn.*, **1**(3), 283-291.

Bathe, K.J. and Noh, G. (2012), "Insight into an implicit time integration scheme for structural dynamics", *Comput. Struct*, **98-99**, 1-6.

Belytschko, T. and Hughes, T.J.R. (1983), *Computational Methods for Transient Analysis*, Elsevier Science Publishers B.V., North-Holland.

Chang, S.Y. (2007), "Improved explicit method for structural dynamics", *J. Eng. Mech.*, ASCE, **133**(7), 748-760.

Chang, S.Y. (2010), "A new family of explicit method for linear structural dynamics", *Comput. Struct.*, **88**(11-12), 755-772.

Chang, S.Y. (2014), "Numerical dissipation for explicit, unconditionally stable time integration methods", *Earthq. Struct.*, **7**(2), 157-176.

Chung, J. and Hulbert, G.M. (1993), "A time integration algorithm for structural dynamics with improved numerical dissipation: the generalized-α method", *J. Appl. Mech.*, **60**(6), 371-375.

Goudreau, G.L. and Taylor, R.L. (1972), "Evaluation of numerical integration methods in elasto-dynamics", *Comput. Meth. Appl. Mech. Eng.*, **2**(1), 69-97.

Hilber, H.M., Hughes, T.J.R. and Taylor, R.L. (1977), "Improved numerical dissipation for time integration algorithms in structural dynamics", *Earthq. Eng. Struct. Dyn.*, **5**(3), 283-292.

Hilber, H.M. and Hughes, T.J.R. (1978), "Collocation, dissipation, and 'overshoot' for time integration schemes in structural dynamics", *Earthq. Eng. Struct. Dyn.*, **6**(1), 99-118.

Newmark, N.M. (1959), "A method of computation for structural dynamics", *J. Eng. Mech. Div.*, ASCE,

85(3), 67-94.
Wood, W.L., Bossak, M. and Zienkiewicz, O.C. (1981), "An alpha modification of Newmark's method", *Int. J. Numer. Meth. Eng.*, **15**(10), 1562-1566.
Zhou, X. and Tamma, K.K. (2006), "Algorithms by design with illustrations to solid and structural mechanics/ dynamics", *Int. J. Numer. Meth. Eng*., **66**(11), 1841-1870.

CC